

Normal and Oblique Impacts of Hard Projectile on Single and Layered Plates—An Experimental Study

V. Madhu and T. Balakrishna Bhat

Defence Metallurgical Research Laboratory, Hyderabad – 500 058

and

N.K. Gupta

Indian Institute of Technology Delhi, New Delhi – 110 016

ABSTRACT

The phenomenon of ordnance velocity impact of projectile on single and layered plates is of interest for many applications. In this paper, an experimental study of normal and oblique impacts of an ogive shaped, hard steel projectile on single and layered plates of mild steel and aluminium is presented. The projectiles were fired at an impact velocity of about 820 ms⁻¹. The plate thickness was varied in the range 10 mm to 40 mm and the ratio of plate thickness to the diameter of the projectile varied in the range 1.5 to 13.0. Observations on target damage and measurements of incident and residual velocities for different angles of impact are presented. Plate thickness t , for which the incident velocity is the ballistic limit, is determined. Computer simulations were carried out using a hydrodynamic code to simulate the normal impact of a projectile and compared these with the experimental results. Experiments were performed to evaluate the response of these plates of intermediate thickness when layered, and the results were compared to the results of single plate of same total thickness.

Keywords: Projectiles, impact, normal impact, oblique impact, plates, simulations, layered plates, target damage, ballistic limit, ballistics, residual velocity, perforation, material hardness, multilayered targets

1. INTRODUCTION

Literature survey on experimental determination and analytical formulation for determining ballistic limit of single plates and the residual velocity of the projectile for incident velocities higher than the ballistic limit has been carried out¹⁻⁴. Quite a few studies on normal impact for plate thickness less than 10 mm have appeared in literature⁵⁻¹¹.

A basic requirement of armour steel is that it should have high hardness; but it was noted¹² that there is no simple correlation between hardness and resistance to perforation, as measured by the structure's ballistic limit. Experiments on multi-layered targets in literature are rather few¹³.

There are relatively few investigations carried out on the oblique impact of rigid projectiles on

targets¹⁴⁻¹⁶. Plots of nondimensional velocity drop against initial obliquity¹⁷ showed that at higher impact velocities, there is little change in the angle of flight of projectile during the penetration process. In an earlier paper¹⁸, the authors have presented the results of an experimental study performed on mild steel plates of various thicknesses. When impacted by *hardcore* projectiles at velocities of about 820 ms⁻¹ and at different angles of obliquity till ricochet occurred in each plate thickness.

In this paper, an experimental study of the normal and oblique impacts of armour piercing projectiles on single and layered plates of mild steel, rolled homogeneous armour (RHA) steel, and aluminium has been presented. The projectiles were fired at an impact velocity of about 800–820 ms⁻¹. The plate thickness varied from 10 mm to 40 mm and the ratio of plate thickness to the diameter of the projectile varied from 1.5 to 6.5 for single plates and up to 13.0 for layered plates.

2. EXPERIMENTAL PROCEDURE

Experiments were performed in small arms range, wherein spinning *hardcore* armour piercing projectiles were fired using a standard rifle. The test setup for impact testing is shown in Fig. 1. Mild steel and aluminium plates were used in the experiments, and the thicknesses and properties materials of these plates are shown in Table 1. To ensure the stability of projectiles, the gun was mounted on a rigid mount with holding devices. The gun

Table 1. Thickness and properties of materials used

Material	Thickness (mm)	Hardness (VPN)	Yield stress (MPa)
Mild steel	10, 12, 16, 20, 25	140-145	327
RHA steel	8, 12, 16, 20	280-300	940
Aluminium	10, 20, 30, 40	30-35	135

was aligned on a level plane. The rifling of the gun imparted spin to the projectile. The projectile core was 6.2 mm in diameter, 27.6 mm in length and weighed 5.2 g. It was ogival in shape and had a copper sheath. The projectile was made of hard steel alloy; its hardness at the tip was about 900 VPN.

The small arms range consisted of a firing chamber, a long tunnel, and an observation chamber. The target-holding fixture was located in the tunnel at 10 m from the gun and could be rotated to hold a plate at any desired angle for oblique impact. All the plates were square shaped and were held to the fixture with C-clamps on their four corners. The stand was then adjusted for the desired angle of impact, which varied from 0° to about 60°. The impact and residual velocities of the projectile were measured in each test using four velocity screens, made of aluminium foils attached to cardboard and fixed on to a wooden frame. These foils were connected to a multichannel electronic timer as shown in Fig. 1. The first two velocity screens were placed at 6 m and 8 m from the muzzle of the gun and the other two velocity screens were placed

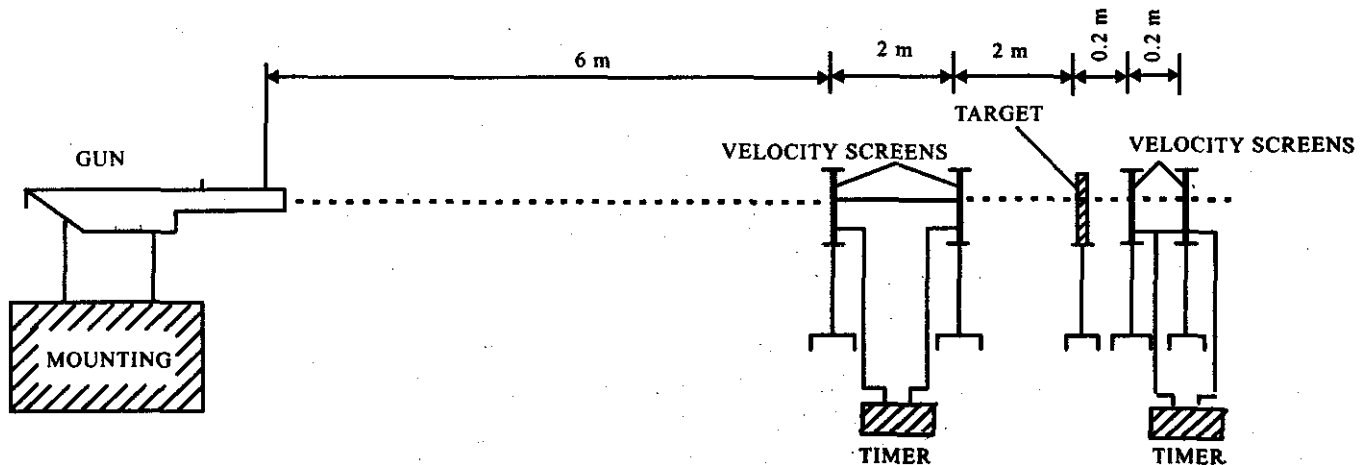


Figure 1. Experimental setup for impact testing

0.2 m and 0.4 m behind the target. In these experiments, the projectiles were recovered after perforation of the target and it was observed that there was no significant deformation of the projectile.

3. NORMAL IMPACT ON SINGLE PLATES

In the experiments, single plates employed were of mild steel of thicknesses 10 mm, 12 mm, 16 mm, 20 mm, and 25 mm, RHA steel of thicknesses 8 mm, 12 mm, 16 mm and 20 mm, and aluminium plates of thicknesses 10 mm, 20 mm, 30 mm, and 40 mm.

Mild steel plates employed in these experiments were all perforated. Post-impact measurements showed that the diameter of the crater was larger at the entry point than at the exit point, and the

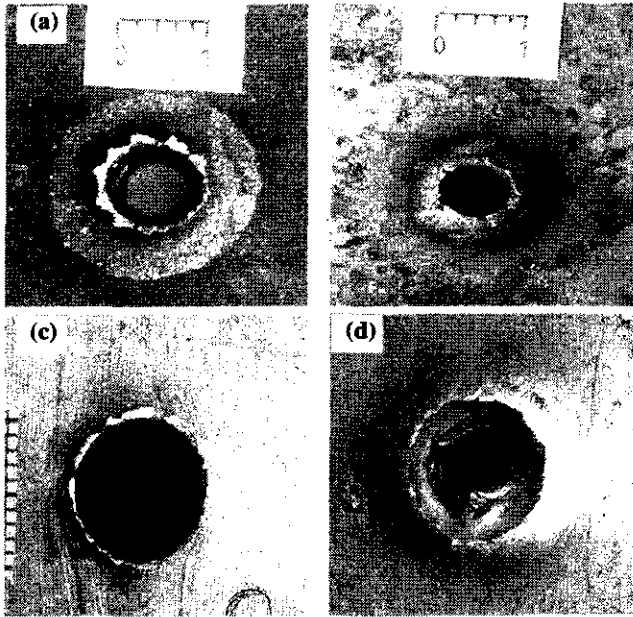


Figure 2. Typical front and rear crater damages in normal impact on (i) 12 mm thick mild steel plate (a) front side and (b) rear side and (ii) 40 mm thick aluminium plate (c) front side, and (d) rear side.

plates showed the formation of petals on their front side and a bulge on the rear side. Figure 2 shows typical front and rear side damages in a 12 mm thick plate under normal impact. The impact and residual velocities of the projectiles were recorded in all the tests and the residual velocities of the projectiles have been plotted against plate thicknesses in Fig. 3.

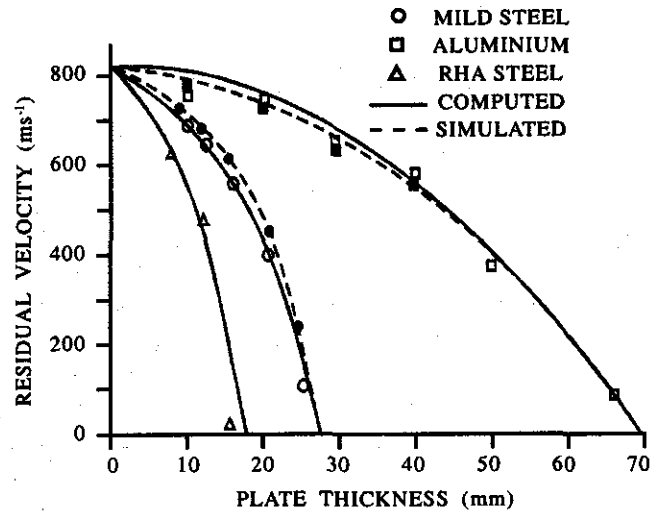


Figure 3. Residual velocity versus plate thickness in normal impact of single plates of mild steel, aluminium, and RHA steel.

RHA steel plates of thicknesses 8 mm and 12 mm employed were perforated. In a 16 mm thick plate, the projectile protruded from the rear side of the plate by about 11 mm. When the projectile was fired on a 20 mm thick plate, it penetrated to a depth of 18 mm and then rebounded back. As in case of mild steel, the front side crater diameter in RHA was larger than the diameter at the rear side.

The aluminium plates employed were all perforated. Crater on the front side of each plate showed the formation of very small petals as compared to the ones formed in mild steel plates, and a light bulge on their rear side. In these plates, the diameters of the craters formed were of larger sizes at the rear sides than those at the front sides. This is quite opposite to the response of mild steel plates where the front side crater diameters were larger. Figure 2 shows the typical front side and rear side damages of 30 mm thick plates of mild steel and aluminium.

3.1 Analysis of Results

From the results of these experiments, it has been found that the residual velocity of the projectile for a normal impact, can be written in the form

$$V_R = V_i - K_1 \cdot t^2 \quad (1)$$

where V_i and V_R are the incident and the residual velocities, t is the plate thickness and K_1 is a function of incident velocity and plate material. The values of K_1 for different materials as determined from experiments are 0.17, 1.05 and 2.53 for aluminium, mild steel, and RHA steel plates, respectively.

From Eqn (1), the ballistic limit thickness (t^*) for which the incident velocity is the ballistic limit, for different materials used may be found by substituting $V_R = 0$ and the respective values of V_i and K_1 as determined above. For $t = t^*$, and $V_R = 0$, from Eqn (1) one gets:

$$t^* = \sqrt{\frac{V_i}{K_1}} \quad (2)$$

The values of t^* were found from Eqn (2) for aluminium, mild steel, and RHA steel as 70 mm, 28 mm and 18 mm, respectively. Now, substituting for K_1 from Eqn (2), Eqn (1) can alternatively be written in the form

$$V_R = V_i [1 - (t/t^*)^2] \quad (3)$$

Residual velocities of projectile for different thicknesses of these plates were computed using Eqn (3) for the respective t^* . These are plotted as firm lines in Fig. 3, and are seen to be in good agreement with the experimental results. Equation (3) is very useful in determining the residual velocity V_R for thickness, $t < t^*$, when the incident velocity, V_i and the plate thickness t^* are known. The hardness of the materials used have been plotted against the respective t^* in Fig. 4.

From these results, t^* has been related to the hardness of the material (denoted as H), by a relation of the form

$$\ln(t^*) = 6.65 - \frac{2}{3} \ln(H) \quad (4)$$

This relation compares well with the present experiments. Equations (3) and (4), when employed together would give the residual velocity in terms of the hardness of the material.

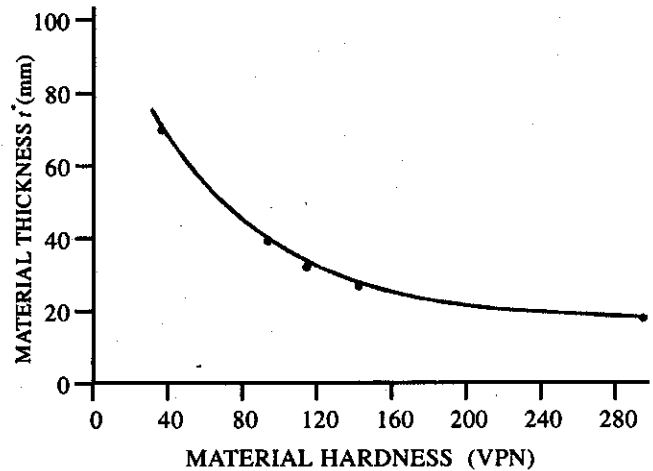


Figure 4. Material hardness versus thickness t^* for which V_i is the ballistic limit.

3.2 Simulation

Computer simulations for the above set of experiments were performed using a 2-D hydrodynamic finite difference code PRHD, which solves material flow problems in the elastic-plastic and hydrodynamic regime. The code solves the equations of continuum mechanics formulated in Lagrangian coordinates. The finite difference operators are centred on time and space to give a second-order accuracy. The code written in Fortran was implemented on Sun Sparc workstation.

Each problem is discretised into a number of small elements called the computational grids. In the finite difference method, spatial and time grids are constructed by replacing derivatives in the governing equations of continuum dynamics with different approximations. Solutions on time are obtained by integration. Equations of motion are expressed directly in terms of pressure gradients of the neighbouring meshes. The regularity of the mesh implicitly establishes the connectivity information. Inaccuracies in numerical approximations grow when the grid distortions are significant, resulting in negative volume and mass, which is overcome using re-zoning and sliding interfaces. Difficulties are encountered in the numerical solutions when shock waves are present. Shock fitting in one dimension can be solved using Rankine-Hugoniot jump conditions. A built-in artificial dissipative term having the form

of viscosity is introduced in the code, to smear the shock over a region. This term, called the artificial viscosity, is of the form

$$q = c_o^2 \rho \Delta r^2 (ds/dt)^2 + c_L \rho \Delta r a | ds/dt | \quad (5)$$

$$q = 0 \text{ for } ds/dt \geq 0 ; a = \sqrt{P/\rho}$$

where ds/dt is the rate of strain in the direction of acceleration, ρ is the density of the medium, Δr is the characteristic grid length, and a is the local sound speed. c_o and c_L are constants¹⁹ with typical values of c_o being 2 and c_L ranging between 0.1 and 0.5.

Von Mises yield criterion has been used in the code to describe the elastic, perfectly plastic material behaviour in terms of the principal stress deviators in the form

$$\sqrt{(s_1 - s_2)^2 + (s_2 - s_3)^2 + (s_3 - s_1)^2} = \sqrt{2} Y^o \quad (6)$$

The flow stress Y^o is not constant for most of the materials but depends on the dynamic condition. A more complete description of the material behaviour is given by a constitutive equation that relates the flow stress to the plastic strain, temperature, and stress state. For a work-hardening material, the stress rate increases with the strain rate beyond the elastic limit. This is introduced in the code in the form of a constitutive relation of the form

$$Y = Y^o [\alpha + \beta \epsilon^p]^n f(C_1, P, V, T) \quad (7)$$

where α , β , n , C_1 are constants, ϵ^p is the equivalent plastic strain, V is the relative volume, P is the pressure, and T is the temperature. The materials are modelled with the Mie-Gruneisen equation of state. The time step for numerical integration is adjusted for optimal computation using a stability criterion. The time step for a given cycle depends on the smallest zone dimension divided by the local sound speed. The above equations form the description of the constitutive equations to model the material behaviour provided in the code.

Using the above formulations that form the basis of the software code, simulations were carried out for the present set of experiments of normal impact on mild steel and aluminium plates. The target and the projectile were first modelled using a pre-processor that generated the information usable by the main processor through a set of well-defined user-friendly commands. All the material parameters needed by the program were taken from the in-built 40 different types of materials library in the code. In the second stage, the main processor performed the integration of the various equations of continuum mechanics using partial differential formulations for each computational time step. The computation in each run was carried out till 150 ms of penetration process and various parameters like residual velocity, depth of penetration, etc. were monitored at every 5 μ s and the histories were dumped in to a file. Using a post-processor, the results of these simulations were analysed and plotted.

The residual velocity of the projectile after complete perforation in different thicknesses of mild steel and aluminium plates have been plotted in Fig. 3. Deformations in the plates during various stages of penetration process were monitored. Figure 5 shows simulation results of deformation in a 12 mm thick mild steel plate. The simulation results match closely with the results obtained analytically and experimentally.

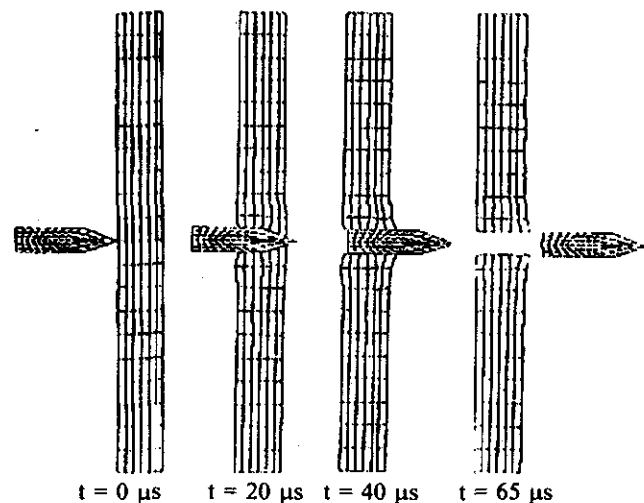


Figure 5. Computer simulation of penetration in a 12 mm thick mild steel plate during normal projectile impact.

4. OBLIQUE IMPACT ON SINGLE PLATES

A study of the oblique impact of projectile on mild steel and aluminium plates has been carried out. In the present experiments, the angle of obliquity was increased gradually from 0° (normal impact) to 60° (oblique impact), or till ricochet occurred in each plate thickness. Measurements of the impact and residual velocities were obtained. The velocity drop in the projectile and its influence on the plate thickness and angle of obliquity of impact have been presented. The influence of plate thickness and the angle of obliquity on both ballistic limit and ricochet have been discussed.

In the present experiments, projectiles were fired at different angles of oblique impact on mild steel plates. In all the different plate thicknesses of mild steel, it was observed that the crater formed after perforation or ricochet, were all elliptical in shape. The impact and residual velocities were measured in each case. From these values the percentage nondimensional velocity drop, as defined by Goldsmith and Finnegan¹⁷, was computed in each case as

$$V_d = \frac{V_i - V_R}{V_i} \times 100 \tag{8}$$

The computed values of velocity drop for various angles of impact and for different plate thicknesses are shown in Fig. 6. The points in Fig. 6, which correspond to 100 per cent velocity drop, give the ballistic limit for each plate thickness.

When the projectile is fired at an angle greater than the angle for ballistic limit, a stage comes when the projectile penetrates the plate and comes out of it from the impacted side itself. The minimum angle at which this occurs is called the critical ricochet angle. Figure 7 shows a photograph



Figure 7. Crater damage in a 12 mm thick mild steel plate due to critical ricochet of projectile.

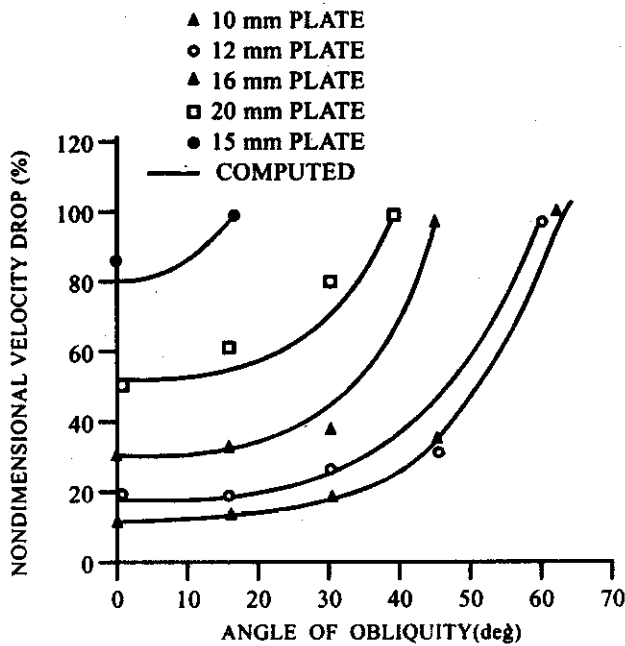


Figure 6. Nondimensional velocity drop as a function of angle of obliquity for different thicknesses of mild steel plates.

of 20 mm thick plate, deformed due to the projectile impacted at angles of critical ricochet (θ_c), which was 51°. When the target plate was impacted at an angle of obliquity greater than θ_c , the projectile ricochet occurred without the penetration taking place, in contrast to the case of critical ricochet where penetration also takes place. It was observed that a stage comes, wherein, when the projectile is fired at angles less than the angle of critical ricochet and greater than the angle at which perforation takes place, the projectile embeds into the target.

Oblique impact studies were also carried out in the present experiments on aluminium plates for angles of obliquity of 0° (normal impact), 30°, 45° and 60° (oblique impacts). It was observed that the projectile perforated all the plate thicknesses at all

the angles of oblique impact till 60° (oblique impacts).

Measurements of the impact and residual velocities were carried out and the nondimensional velocity drop in each case was computed using Eqn (8) and plotted against the angle of impact for different plate thicknesses in Fig. 8. The points in Fig. 8 which correspond to the extrapolated 100 per cent velocity drop gives the ballistic limit for each plate thickness.

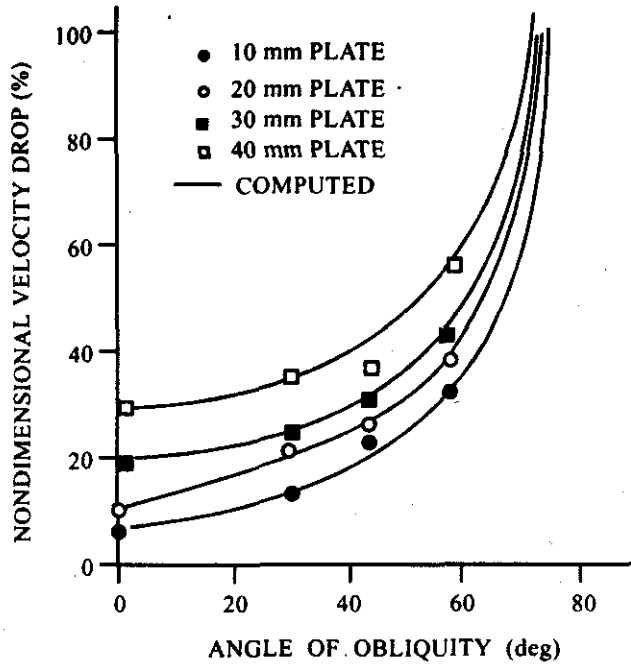


Figure 8. Nondimensional velocity drop as a function of angle of obliquity for different thicknesses of aluminium plates.

4.1 Analysis

In the present experiments on mild steel plates, from the values of the residual velocities, the percentage nondimensional velocity drop in each case is computed using Eqn (8) and plotted against angle of impact for various plate thicknesses as shown in Fig. 6. From these plots, the nondimensional velocity drop V_d , can be written as

$$V_d = \exp(K_2 \theta) + K_3 \quad (9)$$

where θ is the angle of obliquity and K_2 and K_3 are the functions of plate thickness t . The value of K_3 is determined considering that for normal

impact, $q = 0^\circ$, Eqn.(9) becomes:

$$(V_d)_0 = 1 + K_3 \quad (10)$$

where, $(V_d)_0$ is the velocity drop in the normal impact. Now, from Eqn (1), one gets:

$$V_i - V_R = K_1 t^2 \quad (11)$$

or

$$(V_d)_0 = \frac{V_i - V_R}{V_i} \times 100 = \frac{K_1 t^2}{V_i} \times 100 \quad (12)$$

for mild steel, $K_1 = 1.05$ and for $V_i = 820 \text{ ms}^{-1}$

$$(V_d)_0 = 0.128 \times t^2 \quad (13)$$

The points in Fig. 6, which correspond to the 100 per cent velocity drop, give the ballistic limit for each plate thickness. For the present projectile velocity of about 820 ms^{-1} , the angle (in degrees), θ_b , for the ballistic limit to occur in plate of thickness t , is given as

$$\theta_b = K_4 \times \left(\frac{1-t}{t^*}\right)^{1/2} \quad (14)$$

where t^* is the thickness for which the impact velocity V_i is the ballistic limit in the normal impact, i.e., for $\theta_b = 0^\circ$.

For mild steel, it is found that $K_4 = 70^\circ$. Substituting for K_3 from Eqn (10) and for θ_b , the obliquity for ballistic limit for each thickness (for $V_d = 100$ per cent) from Eqn (14), the value of K_2 for each thickness is obtained as

$$K_2 = \frac{\ln(100 - K_3)}{\theta_b} \quad (15)$$

With the help of Eqns (13), (14), and (15), Eqn (9) was solved to give the nondimensional velocity drop for any given thickness for which perforation takes place. The equations are valid up to the thickness for which the impact velocity V_i becomes the ballistic limit. The results, thus

computed for the velocity drop, matched well with the experimental results as shown in Fig. 6.

5. NORMAL IMPACT ON LAYERED PLATES

The results of normal impact on the multi-layered plates available in literature cannot easily be correlated due to varied types of materials, configurations, striker speeds, and geometries used. The question of effectiveness of layering appears to be the subject of some controversy. Experiments were performed to evaluate the response of mild steel and aluminium plates of intermediate thicknesses when layered in comparison to single plate of same total thickness. The results of the penetration resistance of these target systems have been studied and the nature of deformations undergone by the plates have been discussed.

Mild steel plates were put in two layers. The results of residual velocities have been presented in Table 2 which reveal that there is no significant change in the ballistic performance due to layering of such intermediate thicknesses of plates in comparison to equivalent monolithic plate thickness.

A couple of tests were also carried out to study the ballistic performance of layered plates when the combined thickness of the layers exceeded the ballistic limit thickness of the projectile impacted

Table 2. Impact and residual velocities of projectile in normal impact of layered plates

Material	Total thickness (mm)	Layer Config	Impact velocity (ms ⁻¹)	Measured residual velocity (ms ⁻¹)	Computed* residual velocity (ms ⁻¹)
Mild steel	20.0	10+10	826.8	410.0	405.1
	26.0	10+16	820.1	113.2	112.9
	26.0	16+10	833.1	117.3	114.7
	30.0	10+20	821.0	Embed	-
	30.0	20+10	811.9	Rebound	-
	36.0	16+20	812.0	Embed	-
	36.0	20+16	805.7	Rebound	-
	37.0	25+12	810.3	Rebound	-
	Aluminium	50.0	30+20	832.8	386.9
66.0		33+33	835.5	102.4	93.2
80.0		20+30+30	831.6	0.0	-

* Computed using Eqn (3)

at the present velocity ranges, and also the effect of keeping thinner or thicker layer in the front. It was observed that when the impacted front side had a thinner plate than the rear side plate, the projectile got embedded into the plates, whereas, when the same configuration was reversed, i.e. by placing the thicker plate in the front side and the thinner one on the rear side, the projectile penetrated to about 28-29 mm and then rebounded back. When a 10+20 combination was impacted, the projectile penetrated 28.9 mm and got embedded in the target, whereas, when the same combination was reversed to 20+10, the projectile penetrated to 29.6 mm and then rebounded back. The phenomena is due to the stress wave effects and is quite interesting for further investigations.

Aluminium plates of thicknesses 20 mm, 30 mm, and 33 mm were put in two and three layers in contact. The impact and residual velocities of the projectile are presented in Table 2. The aim of these experiments is to see the efficacy of layering such thickness, on the ballistic performance of the layered system. The results reveal that there is no significant change in the ballistic performance due to layering of such intermediate thickness of plates.

6. CONCLUSIONS

Armour piercing projectiles were fired normally and at oblique angles on single and layered plates of mild steel, RHA steel, and aluminium. Measurements of the impact and residual velocities and the crater damages observed have been presented. An analysis of the results of the impacts on single plates leads to a simple equation for determining the residual velocity when the ballistic limit thickness t^* is known. The results of the residual velocities obtained from the developed relation compare well with the experiments. The thickness t^* has also been related to the hardness of the material. Results of residual velocity of projectile obtained from computer simulations of normal impact on mild steel and aluminium plates were observed to be close to the experimental results.

Experiments were also performed on single plates by increasing the obliquity of impact for each plate thickness until ricochet occurred. Velocity

drop curves are presented and relations between velocity drop, thickness of plate, and angles of obliquity valid up to ballistic limit, are developed.

In layered plates of mild steel, it was found that the projectile after penetrating about 28 mm to 30 mm, rebounded back in the direction opposite to its direction of initial flight before impact when a thicker plate was kept in the front side and a thinner plate on the rear side of a two-layer configuration. The residual velocities after perforation of combined target in plates of intermediate thicknesses were of the same order as in the case of monolithic target.

ACKNOWLEDGEMENTS

The authors thank Shri K.K. Papukutty, Scientist, and staff of Small Arms Range of Defence Metallurgical Research Laboratory (DMRL), Hyderabad, for their help in carrying out the experiments.

REFERENCES

1. Goldsmith, W. Non ideal projectile impact on targets. *Int. J. Impact Engg.*, 1999, **22**, 95-395.
2. Backman, M.E. & Goldsmith, W. The mechanics of penetration of projectiles into targets. *Int. J. Engg. Sci.*, 1978, **16**, 1-99 .
3. Zukas, J.A. High velocity impact dynamics. John Wiley & Sons, 1990.
4. Corbett, G.G.; Ried, S.R. & Johnson, W. Impact loading of plates and shells by free-flying projectiles: A review. *Int. J. Impact Engg.*, 1996, **18**, 141-30.
5. Landkof, B. & Goldsmith, W. Petalling of thin metallic plates during penetration by cylindro-conical projectiles. *Int. J. Solids Struct.*, 1983, **21**, 245-66.
6. Leppin, S. & Woodward, R.L. Perforation mechanisms in thin titanium alloy targets. *Int. J. Impact Engg.*, 1986, **4**, 107-15.
7. Corran, R.S.J.; Shadbolt, P.J. & Ruiz, C. Impact loading of plates—an experimental investigation. *Int. J. Impact Engg.*, 1983, **1**, 3-22.
8. Palomby, C. & Stronge, W.J. Blunt missile perforation of thin plates and shells by discing. *Int. J. Impact Engg.*, 1988, **7**, 85-100.
9. Levy, N. & Goldsmith, W. Normal impact and perforation of thin plates by hemispherically tipped projectiles. *Int. J. Impact Engg.*, 1984, **2**, 299-24.
10. Calder, C.A. & Goldsmith, W. Plastic deformation and perforation of thin plates resulting from projectile impact. *Int. J. Solids Struct.*, 1971, **7**, 863-81.
11. Beynet, P. & Plunkett, R. Plate impact and plastic deformation by projectiles. *Experimental Mechanics*, 1971, **11**, 64-70.
12. Sangoy, L.; Meunier, Y. & Pont, G. Steels for ballistic protection. *Israel J. Tech.*, 1988, **24**, 319-26.
13. Radin, J. & Goldsmith, W. Normal projectile penetration and perforation of layered targets. *Int. J. Impact Engg.*, 1988, **7**, 229-59.
14. Zaid, M. & Paul, B. Oblique perforation of a thin plate by a truncated conical projectile. *J. Franklin Inst.*, 1959, **268**, 24-45.
15. Woodward, R.L. & Baldwin, N.J. Oblique perforation of targets by small armour piercing projectiles. *J. Mech. Engg. Sci.*, 1979, **21**, 85-91.
16. Virostek, S.P.; Dual, J. & Goldsmith, W. Direct force measurements in normal and oblique impact of plates by projectiles. *Int. J. Impact Engg.*, 1987, **6**, 247-69.
17. Goldsmith, W. & Finnegan, S.A. Normal and oblique impact of cylindro-conical and cylindrical projectiles on metallic plates. *Int. J. Impact Engg.*, 1986, **4**, 83-105.
18. Gupta, N.K. & Madhu, V. Normal and oblique impact of a kinetic energy projectile on mild steel plates. *Int. J. Impact Engg.*, 1992, **12**, 333-44.
19. Reiner, M. Twelve lectures on theoretical rheology, North Holland Pub Co, Amsterdam, 1949.

Contributors



Dr V Madhu obtained his PhD in Applied Mechanics from the Indian Institute of Technology (IIT) Delhi, New Delhi, in 1993. He worked as Postdoctoral Research Fellow at the University of California, Los Angeles, USA, during 1997-98. Presently, he is working as Scientist E at the Defence Metallurgical Research Laboratory (DMRL), Hyderabad. He has been working in the design and development of advanced armour for battlefield systems since 1982. He has published/presented more than 25 research papers in journals and conference proceedings.

Dr T Balakrishna Bhat obtained his PhD in Metallurgy from the IIT Madras, Chennai, in 1981. He worked as Postdoctoral Research Fellow at the NASA's Jet Propulsion Laboratory, USA, during 1987-90. He is working as Scientist G at the DMRL and currently heading the Armour Design and Development Division of DMRL. He has 25 years of research experience in the areas of high technology materials, including composites, micro-sandwich cellular solids, and advanced armour designs. He has more than 70 research papers and a patent to his credit. He has received four *NASA Invention Cash Awards*, *Best National Metallurgist Award* (1993) and *VASAVIK Award* (1981).